Microstructures and Tensile Mechanical Properties of Titanium Rods Made by Powder Compact Extrusion of a Titanium Hydride Powder

YIFENG ZHENG, XUN YAO, JIAMIAO LIANG, and DELIANG ZHANG

Nearly fully dense titanium with good mechanical properties was fabricated rapidly by induction heating, holding, and hot extrusion of the TiH_2 powder compacts. The dehydrogenation and consolidation processes took less than 15 minutes in total. The microstructures, contents of interstitial elements (H, O), tensile mechanical properties, and fracture behaviors of titanium samples made with different holding and extrusion temperatures [1273 K, 1373 K, and 1473 K (1000 °C, 1100 °C, and 1200 °C)] were investigated. The results showed that the hydrogen content in the extruded rods was around 0.09 wt pct when the holding and extrusion temperature was 1373 K or 1473 K (1100 °C or 1200 °C), with almost all of the TiH_2 phase being transformed into Ti phase during the heating, holding, and extrusion process steps. The extruded Ti samples had a lamellar structure consisting of fine α lamellae with random orientations in different lamellar colonies and the relative density of all the extruded samples exceeded 99.5 pct. The residual TiH_2 phase can reduce the ductility of extruded rods. The sample extruded at 1373 K (1100 °C) has the best elongation to fracture of 21.0 pct, and its average yield strength and ultimate tensile strength reached 536.8 and 691.8 MPa, respectively.

DOI: 10.1007/s11661-016-3333-x

I. INTRODUCTION

TITANIUM and its alloys are regarded as promising engineering materials for many applications in aeronautical, marine, biomedical, chemical, and other industries due to their excellent properties mainly including high strength-to-density ratio, excellent corrosion resistance, outstanding biocompatibility, low thermal expansion coefficient, and a broad service temperature range.[1–3] However, the cost of titanium and titanium alloys is high due to the relatively large amount of energy consumed in producing titanium sponge and titanium powder with a low level of impurity and the relatively high cost of remelting, casting, and thermomechanical processing used to produce titanium mill products (bars, plates, rods, *etc.*). The high cost limits the commercial applications of titanium and titanium alloys to mostly those industries with a relatively low-cost sensitivity such as aerospace, military, and biomedical industries.

One of the fabrication processes that can reduce the cost of titanium and titanium alloy products is powder metallurgy (PM) which could minimize the wastage of raw material and reduce the amount of machining. The most common method for producing low-cost titanium powder used in PM is a hydrogenation–dehydrogenation (HDH) process in which titanium sponge is hydrogenated to form brittle TiH_2 pieces which are subsequently crushed into fine powder particles and then the powder particles are dehydrogenated in vacuum at temperatures above 573 K (300 °C) to obtain a titanium powder.[4,5] In recent years, researchers found that the cost of making titanium and titanium alloy components and structural members can be further reduced by taking a TiH_2 powder instead of an HDH titanium powder as the starting material and some research works on this have been reported.[6–10] Pascu *et al.*[11] obtained fully dense Ti samples by spark plasma sintering (SPS) of a TiH_2 powder at 1373 K (1100 °C) for 10 minutes. Kim *et al.*[12] prepared fully dense nanostructured Ti samples with an average grain size of 80 nm by pulsed-current activated sintering of nanostructured TiH_2 powder produced by high-energy mechanical milling. Luo *et al.*[13] fabricated Ti samples by microwave sintering of TiH_2 powder, and found that the Ti samples had a higher density, finer residual pores, and better mechanical properties than those made by sintering of HDH Ti powder in an electric furnace at the same temperature and for the same time. Chen *et al.*[14] synthesized bulk porous NiTi alloy samples by sintering a mixture of Ni and TiH_2 powders, and observed that the samples exhibited a higher fracture strength, higher pseudoelastic strain, and lower secant modulus compared with the Ni/Ti sintered samples.

In the present study, we fabricated nearly fully dense titanium samples using a TiH_2 powder and a novel powder consolidation process which involves induction heating of a TiH_2 powder compact followed by powder compact extrusion. This powder consolidation process takes less than 15 minutes in total. To elucidate the

YIFENG ZHENG and XUN YAO, Ph.D. Students, JIAMIAO LIANG, Engineer, and DELIANG ZHANG, Professor, are with the State Key Laboratory for Metal Matrix Composites, School of Materials Science and Engineering, Shanghai Jiao Tong University, Shanghai 200240, China. Contact e-mail: zhangdeliang@sjtu.edu.cn
Manuscript submitted May 12, 2015.
Article published online January 22, 2016

influence of holding and extrusion temperature, we studied the microstructures, oxygen and hydrogen contents, tensile mechanical properties, and fracture behaviors of the consolidated samples produced using three different holding and extrusion temperatures.

II. EXPERIMENTAL

The TiH_2 powder used in the study was supplied by Baoji Yutong metal materials Co., Ltd, PR China, and had irregular and equiaxed particle shapes with 99.5 wt pct purity and particle sizes of −200 mesh, as shown in Figure 1(a). The particle size distribution of the as-received powder was measured using Malvern Mastersizer 2000 laser instrument to be D10:8.3, D50:38.9, and D90:83.4 μm, as shown in Figure 1(b). As shown by the XRD pattern in Figure 1(c), the TiH_2 powder consisted of only δ-phase which has an FCC structure. For each sample, 50 g TiH_2 powder was pressed into a powder compact by uniaxial die-pressing at room temperature with a pressure of 500 MPa and a holding time of 5 minutes. The dimensions of the powder compacts were 28 mm in diameter and around 25 mm in height. Then, the powder compacts were induction heated to 1273 K, 1373 K, and 1473 K (1000 °C, 1100 °C, and 1200 °C) with a heating rate of 150 K/min and held at the respective temperature for 5 minutes. Subsequently, the induction sintered powder compacts were hot extruded with an extrusion ratio of 9:1, and the extruded rods were left to be cooled down to room temperature. The stainless steel extrusion cylinder and die were heated to 773 K (500 °C) before the extrusion was performed. The powder compact heating and extrusion were performed in an argon atmosphere in a glove box with an oxygen content of less than 200 ppm to prevent oxidation. Figure 2 shows the schematic diagram of the experimental set-up used in this work.

The oxygen and hydrogen contents of the extruded rods were analyzed using LECO TCH-600 nitrogen/oxygen/hydrogen analyzer. Dog-bone-shaped tensile test specimens with a gage length of 20 mm, a thickness of 2 mm, and a width of 3 mm along the extrusion direction were cut from the extruded rods using electrical discharge machining (EDM) wire-electrode cutting machine. The tensile testing was conducted using a Zwick BTC-T1-FR020TN A50 universal testing machine at room temperature with a strain rate of 5×10^{-4} s^{-1}. All the tensile test specimens were cut from the central region of the extruded rods, and three tensile tests were done for each extruded rod. The fracture surfaces and longitudinal sections below the fracture surfaces of the tensile test specimens were examined using an FEI NOVA NanoSEM 230 scanning electron microscope (SEM). The microstructures of the extruded rods were characterized using OLMPUS BX51M optical microscope, Rigaku Ultima IV X-ray diffractometer (XRD) with Cu Kα radiation, and JEM-2010F transmission electron microscope (TEM). The TEM specimens were prepared by jet-polishing with an electrolyte consisting of 6 pct perchloric acid, 34 pct butyl alcohol, and 60 pct methanol by volume at the temperature of 248 K (−25 °C) and a voltage of 25 V. The ground and polished surfaces of the samples were etched with Kroll's reagent (2 ml HF, 4 ml HNO_3, and 100 ml H_2O) for 10 seconds for examination using the optical microscope.

III. RESULTS

Figure 3 shows the XRD patterns of the rods extruded at 1273 K, 1373 K, and 1473 K (1000, 1100, and 1200 °C) (named as Ti-1273, Ti-1373, and Ti-1473 rods, respectively). The Ti-1273 rod contained mostly α titanium and a small amount of TiH_2 corresponding to the peak with $2\theta = 40.97°$, showing that the dehydrogenation was near completion at 1273 K (1000 °C). When the holding and extrusion temperature increased to 1373 K and 1473 K (1100 °C and 1200 °C), there were no diffraction peaks of TiH_2 in the XRD patterns and the Ti-1373 and Ti-1473 rods only contained α titanium. It was also found that the intensity of the {0002} diffraction peak was clearly stronger than the other peaks in the XRD pattern of the Ti-1273 rod, suggesting that the Ti-1273 rod has some degree of {0002} texture parallel to the extrusion direction. The intensity of this texture increased with increasing the holding and extrusion temperature from 1273 K to 1473 K (1000 °C to 1200 °C).

As shown in Table I, the oxygen content of the Ti-1273 rod was 0.28 wt pct, clearly lower than that of the TiH_2 powder used (0.4 wt pct). Then the oxygen content increased slightly to 0.32 and 0.36 wt pct with increasing the holding and extrusion temperature to 1373 K and 1473 K (1100 °C and 1200 °C). The hydrogen content of the Ti-1273 rod was 0.28 wt pct, which was much lower that in the TiH_2 powder used (3.32 wt pct), showing that most hydrogen has been removed during the short process of induction heating and holding at 1273 K (1000 °C), in agreement with the result of the XRD analysis of the Ti-1273 rod. Then the hydrogen content decreased more significantly to 0.09 wt pct when the holding and extrusion temperature increased to 1373 K (1100 °C), but did not decrease further when the extrusion temperature increased from 1373 K to 1473 K (1100 °C to 1200 °C).

As shown by the optical microscopy images of the etched transverse and longitudinal sections of the as-extruded rods in Figure 4, all the as-extruded rods had a typical lamellar structure. With increasing the extrusion temperature from 1273 K to 1473 K (1000 °C to 1200 °C), the thickness of the α lamellae increased from 0.2-1 to 5-8 μm, and the sizes of the lamellar colonies increased from 50-60 to 120-150 μm. The morphologies and sizes of the lamellar colonies in the microstructures of the extruded rods looked similar in transverse and longitudinal sections, respectively, showing that the prior β grains from which the α lamellae formed were equiaxed rather than elongated after extrusion. This clearly shows that dynamic recrystallization of the β phase driven by plastic deformation occurred during the extrusion process prior to the phase transformation from β phase to α phase.

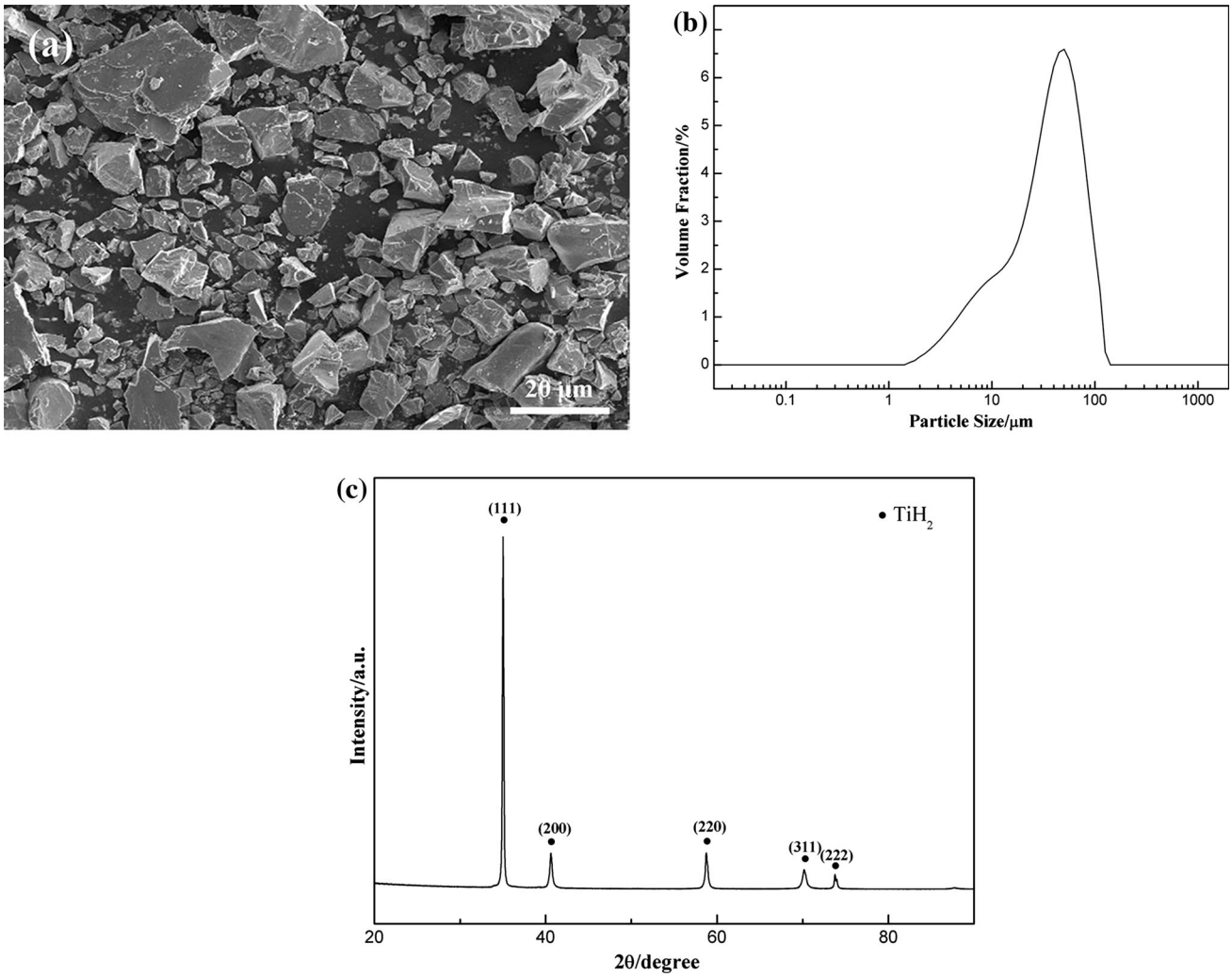

Fig. 1—(*a*) Morphology of the TiH_2 powder particles used; (*b*) particle size distribution of the TiH_2 powder used; and (*c*) XRD pattern of the TiH_2 powder used.

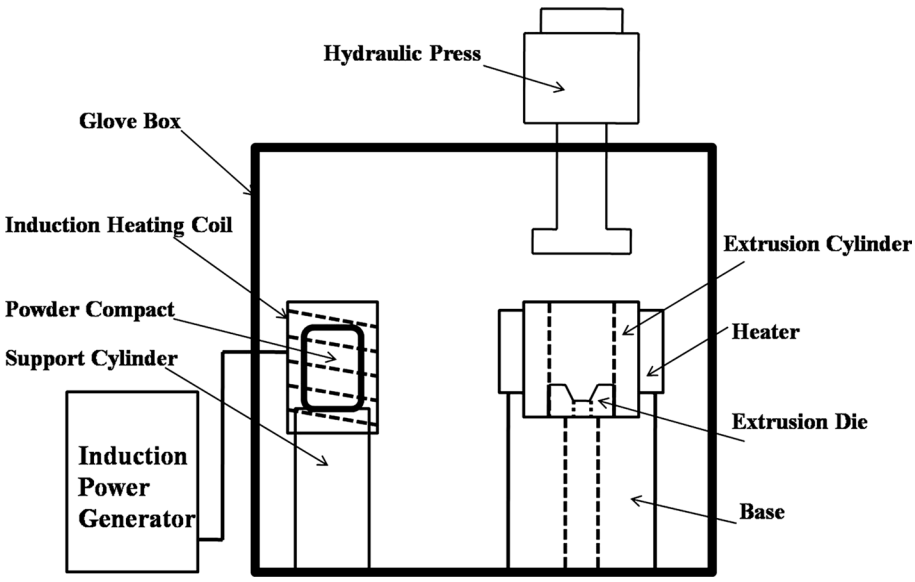

Fig. 2—Schematic diagram of the experimental set-up.

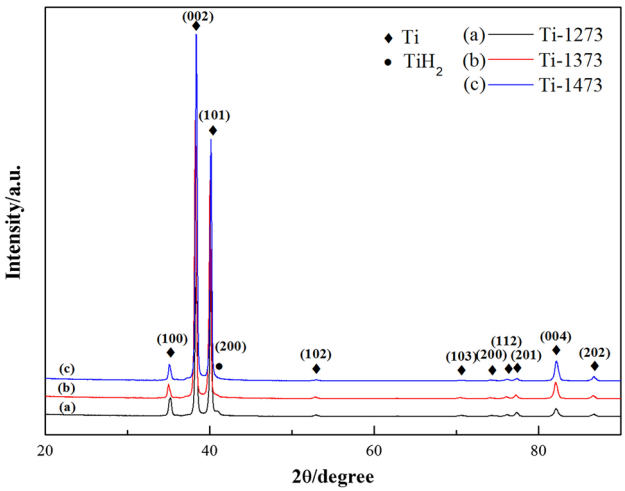

Fig. 3—XRD patterns of the as-extruded rods: (*a*) Ti-1273, (*b*) Ti-1373, and (*c*) Ti-1473.

Table I. Oxygen and Hydrogen Contents of the TiH_2 Powder Used and the As-Extruded Rods

Sample	Oxygen (Weight Percent)	Hydrogen (Weight Percent)
TiH_2 powder	0.4	3.32
Ti-1273	0.28	0.28
Ti-1373	0.32	0.09
Ti-1473	0.36	0.09

Figures. 5 through 7 show the TEM images of the microstructures of the extruded rods made with different holding and extrusion temperatures. As shown in Figure 5, the microstructure of the Ti-1273 rod consisted of mostly α lamellae (area (c)) together with a small fraction of β lamellae (area (d)) and TiH_2 plates (area (e)) distributed among the α lamellae with a thickness in the range of 0.2 to 0.8 μm. The amount of the β lamellae in the Ti-1273 rod was low, and this could be the reason why it was not detected by the XRD analysis. The observation of TiH_2 plates (area (e)) was in agreement with the XRD analysis of the Ti-1273 rod (Figure 3). As shown in Figure 6, the TEM examination of the microstructure of the Ti-1373 rod showed that the thickness of α lamellae (area (d) and (e)) increased to be greater than 1 μm, and there were still a small fraction of β lamellae (area (c)) existing between the α lamellae. Because the H content in this sample is much less compared with that of Ti-1273, the amount of TiH_2 was quite little and no TiH_2 plates were detected in these TEM specimens of this sample. As shown in Figure 7, the microstructure of the Ti-1473 rod almost entirely consisted of the larger α titanium lamella (area (b) and (c)) together with a very small fraction of TiH_2 (area (d)) plates existing at the boundaries between the lamellar colonies, suggesting that there was still some TiH_2 phase which did not decompose even if the holding and extrusion temperature increased to 1473 K (1200 °C). This is in line with the small amount of residual hydrogen of the sample shown by the results of the chemical analysis in Table I. The amount of TiH_2 in the Ti-1473 rod was very small, which made it not detectable by XRD analysis.

All the extruded rods had high relative densities, being 99.6, 99.8, and 99.7 pct for the Ti-1273, Ti-1373, and Ti-1473 rods, respectively, as measured using the Archimedes method. However, as shown in Figure 8, the SEM examination of the polished and un-etched transverse cross sections of the extruded rods showed that there were still a very small fraction of small and round cavities with the sizes in the range of 1 to 4 μm existing in the as-extruded rods.

Figure 9 shows the tensile engineering stress–strain curves of the as-extruded rods, and the average values of their yield strength (YS), ultimate tensile strength (UTS), and elongation to fracture (EL) are listed in Table II. The Ti-1273 rod had the highest average YS and UTS of 595.3 and 726.6 MPa, respectively, but the lowest ductility (EL: 5.4 pct). Then, the YS and UTS of the Ti-1373 rod were clearly lower, being 536.8 and 691.8 MPa, respectively, but the ductility improved drastically, with the EL reaching 21.0 pct. The YS and UTS of the Ti-1473 rod were similar to those of Ti-1373 rod, being 529.3 and 673.8 MPa, respectively, but its ductility fell slightly (EL: 16.7 pct).

As shown in Figure 10(a), the fracture surfaces of the tensile test specimens cut from the Ti-1273 rod were rugged and translamellar, showing delamination of the lamella, features of terraced crack propagation, and small dimples. Micro-cracks were also observed in some lamellae, as indicated by the circles in Figure 10(b), and this illustrated that these lamellae were quite brittle. As shown in Figure 10(c), the fracture surfaces of the tensile test specimens cut from the Ti-1373 rod were rougher and the lamellar delamination was more obvious than those of the Ti-1273 rod. It was also observed that a higher degree of plastic deformation of the lamellae occurred, as evidenced by the larger number of small dimples and larger cavities existing on the fracture surfaces, as shown in Figure 10(d). As shown in Figure 10(e), the fracture surfaces of the tensile test specimens cut from the Ti-1473 rod were generally similar to those of the Ti-1373 rod, but some regions of the fracture surfaces were quite flat, as indicated by the circle in Figure 10(e), which shows that some of the thick α plates had low ductility.

As shown in Figure 11, the longitudinal cross sections of the three tensile test specimens below the fracture surfaces cut from the extruded rods did not show any cavities formed by enlarging the preexisting cavities or separating powder particle surfaces at weakly bonded interparticle boundaries. In line with the observation of the fracture surfaces of the tensile test specimens shown in Figure 10, the profiles of the fracture surfaces also showed that the fracture surfaces of the tensile test specimens cut from the Ti-1273 rod were clearly flatter than those of the tensile test specimens cut from the Ti-1373 and Ti-1473 rods.

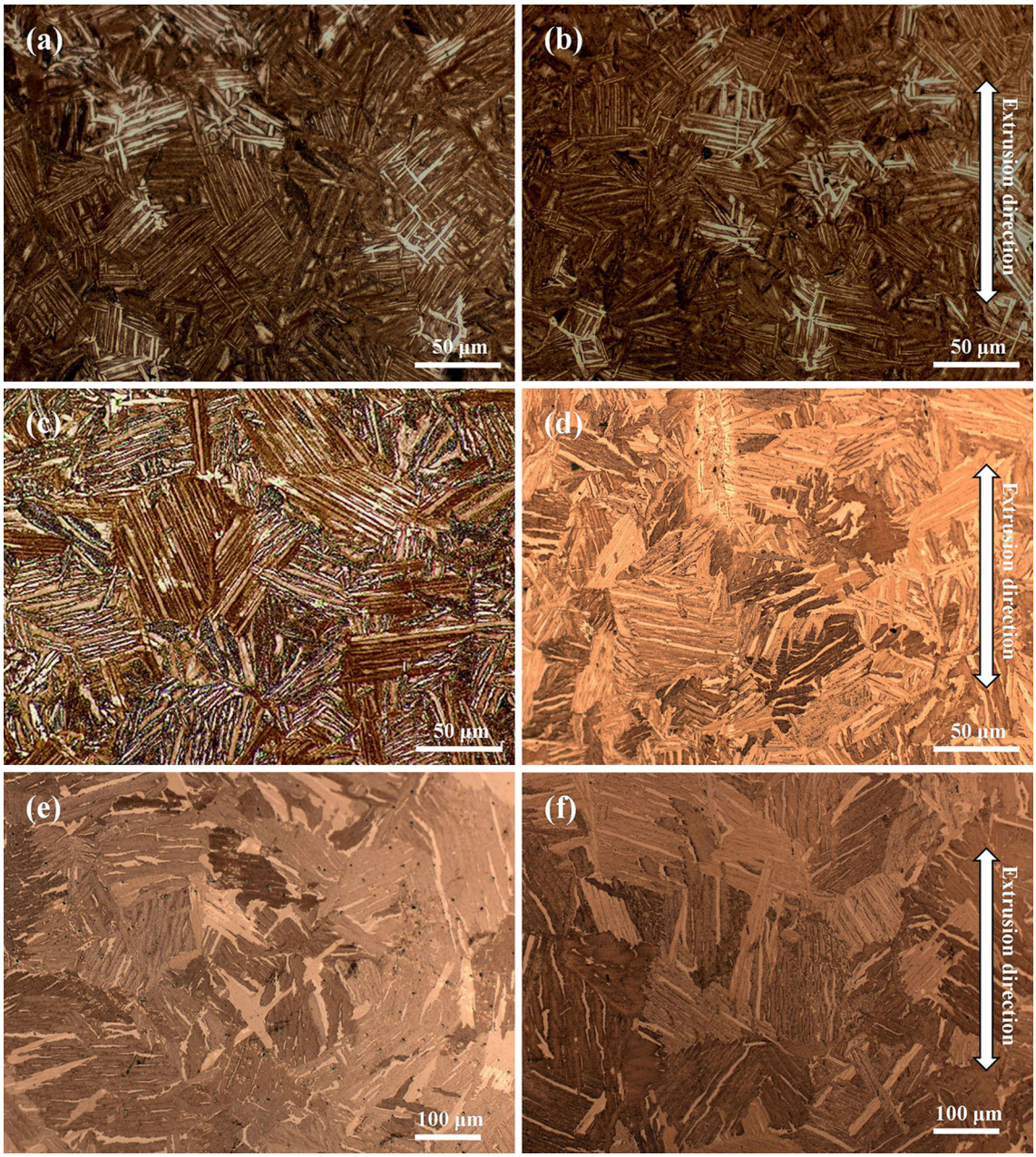

Fig. 4—Optical microscopy images of the etched transverse sections (*a*, *c*, and *e*) and longitudinal sections (*b*, *d*, and *f*) of the Ti-1273 (a and b), Ti-1373 (c and d), and Ti-1473 (e and f) rods.

IV. DISCUSSION

A. *Effect of Holding and Extrusion Temperature on Oxygen and Hydrogen Contents*

As shown in Table I, all the as-extruded rods have a lower oxygen content than that in the starting TiH_2 powder, showing that the oxygen is partly removed during powder compact heating and holding process. The likely mechanisms of the oxygen removal might be that a reaction between the surface titanium oxide film and hydrogen occurs during the dehydrogenation process. Ivasishin *et al.*[15] pointed out that oxygen in TiH_2 powder mainly exists in the surface titanium oxide films covering the particle surfaces, and the surface titanium oxide films could be partially reduced by the released hydrogen during the heating process, resulting in a decrease of the oxygen content in the extruded rods. The present work also shows that with increasing the heating and holding temperature from 1273 K to 1473 K (1000 °C, 1200 °C), the oxygen content slightly rises, most likely due to the presence of oxygen in the argon atmosphere which has been controlled with an oxygen content of <200 ppm. Titanium has a high affinity to oxygen, especially at elevated temperatures, so after the

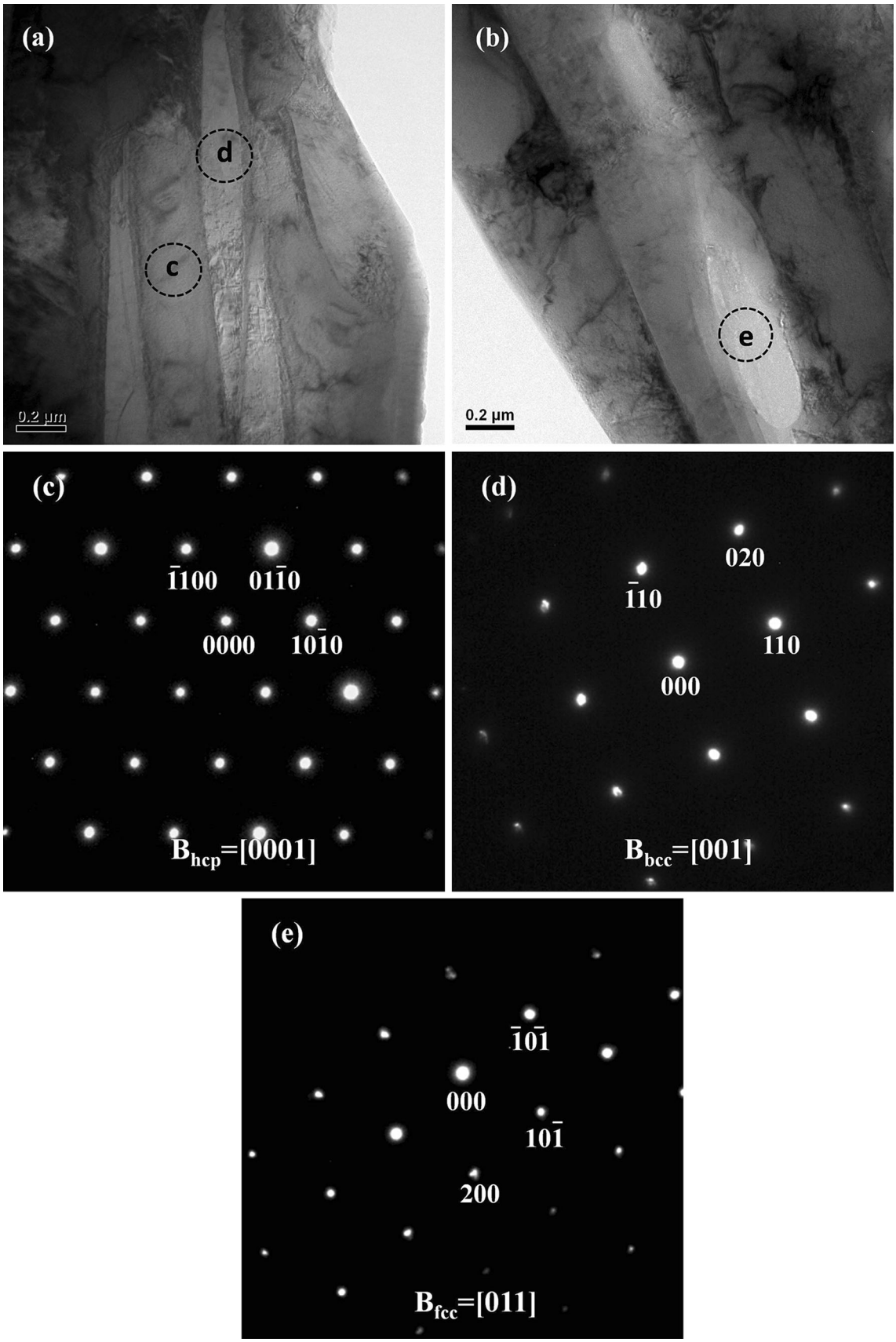

Fig. 5—(*a*) and (*b*) Bright-field TEM images of the microstructure of the Ti-1273 rod; (*c*) through (*e*) SAED patterns of the lamella labeled in (a) and (b).

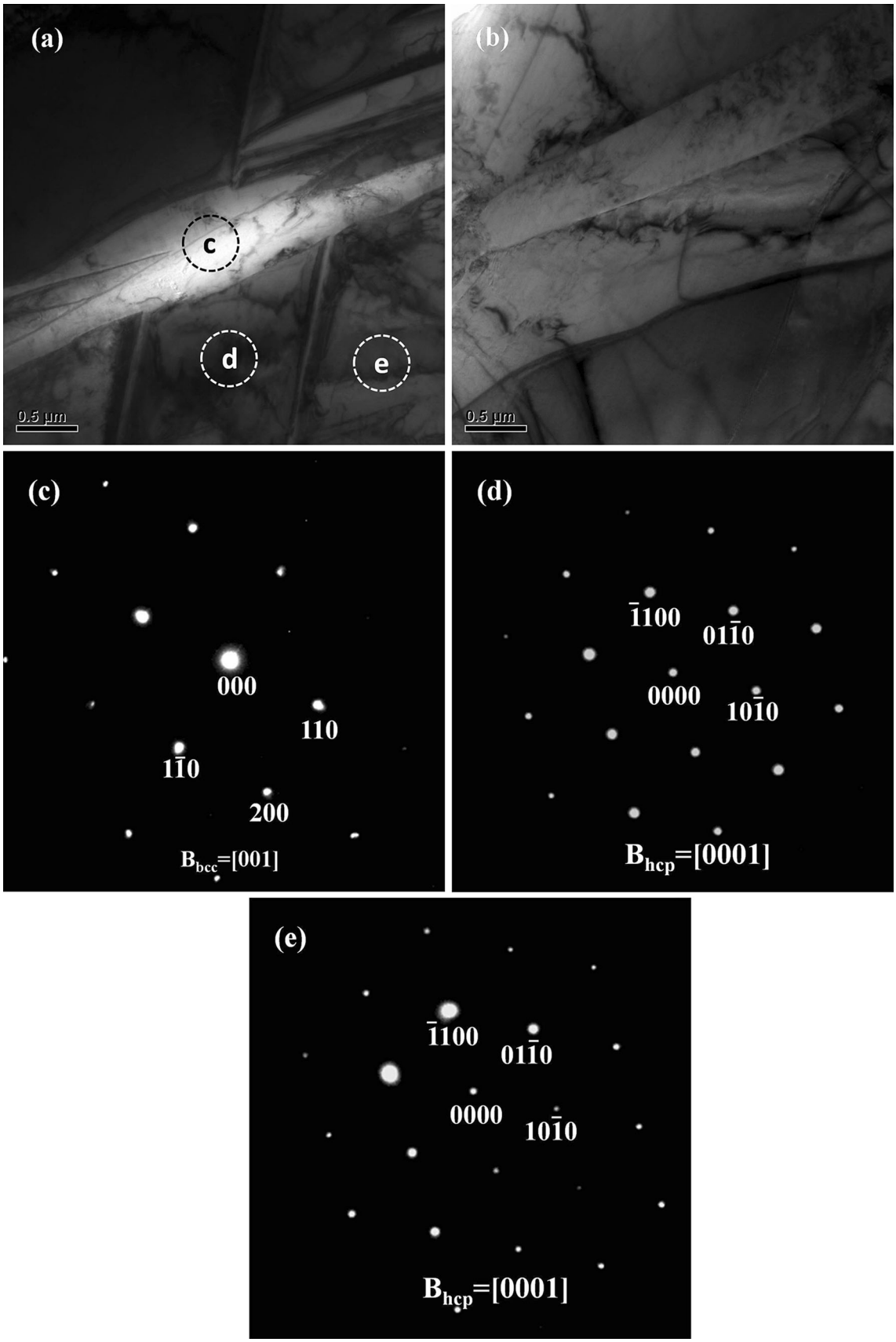

Fig. 6—(*a*) and (*b*) Bright-field TEM images of the Ti-1373 rod; (*c*) through (*e*) SAED patterns of lamella labeled in (a).

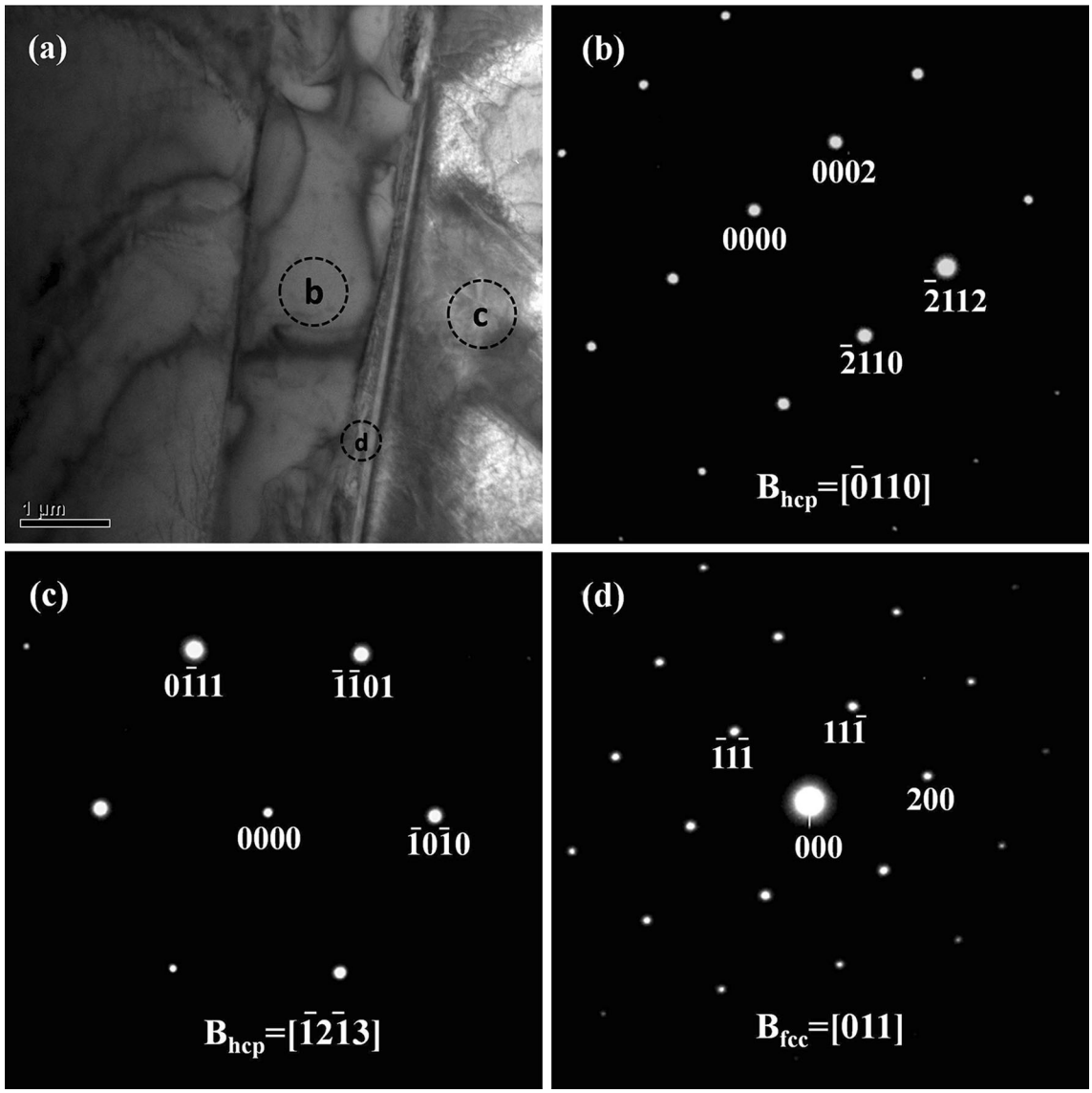

Fig. 7—(*a*) Bright-field TEM image of Ti-1473 rod; (*b*) through (*d*) SAED patterns of lamella labeled in (a).

hydrogen is almost completely removed through dehydrogenation during heating, the oxygen in the atmosphere can diffuse into the lattice of titanium, causing the oxygen content of the powder compact to increase. Since it takes a longer time to heat the powder compacts to a higher temperature, more oxygen is taken from the atmosphere by the powder compact during heating for producing the Ti-1473 rod compared with the samples that extruded at lower temperatures.

From Table I, it can also be found that the hydrogen in the TiH_2 can be completely removed by the induction heating to 1273 K (1000 °C) and holding at this temperature for a short time of 5 minutes. This shows that dehydrogenation of the TiH_2 powder compact in this process was rather rapid, and similar result also has been reported by Kim *et al.*[12] who obtained nanostructured Ti by pulsed-current activated heating of a mechanically activated TiH_2 powder to 1293 K (1020 °C) within 2 minutes. On the other hand, the present study also shows that heating to 1273 K (1000 °C) and holding at this temperature for 5 minutes are insufficient for complete removal of hydrogen, as evidenced by the small amount of TiH_2 detected by both XRD analysis (Figure 3) and TEM examination (Figure 5(b)). This suggests that it takes more than 5 minutes to diffuse all the hydrogen from the internal region of the TiH_2 powder compact at this temperature. When the powder compact is heated to 1373 K (1100 °C) and held at this temperature for 5 minutes, the hydrogen content in the powder compact is reduced significantly to a very low level of 0.09 wt pct, and the hydrogen does not decrease further when the temperature increases to 1473 K (1200 °C), as shown in Table I. This suggests that it is necessary and sufficient to heat the powder compact to 1373 K or 1473 K (1100 °C or 1200 °C) for almost complete dehydrogenation and the dehydrogenation would not be improved continuously with the increasing holding temperature. Previous works[13,16,17] have shown that dehydrogenation of TiH_2 powder in vacuum at temperatures in the range

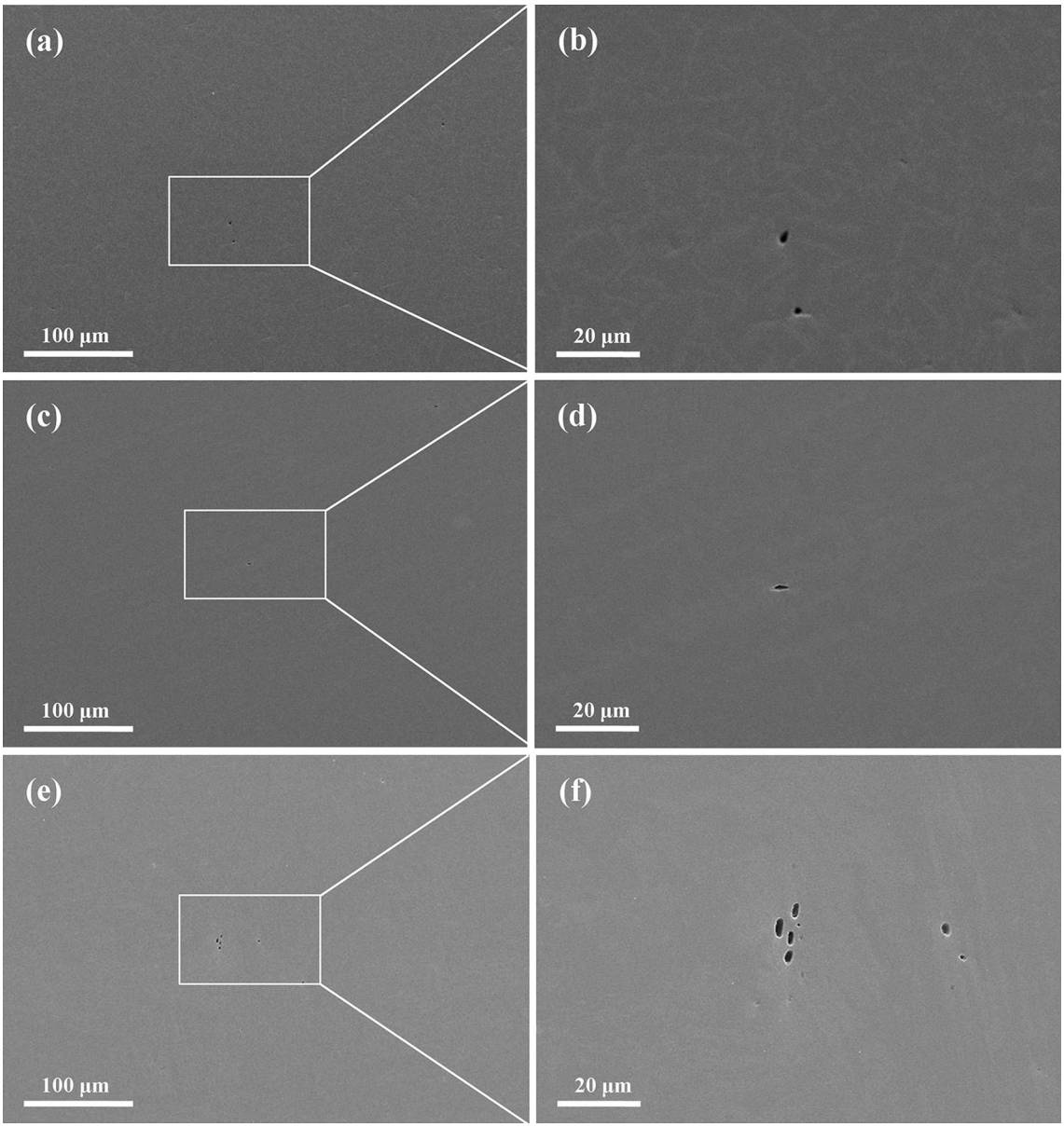

Fig. 8—SEM images of the polished and un-etched transverse section of the as-extruded rods: (*a*) and (*b*) Ti-1273, (*c*) and (*d*) Ti-1373, and (*e*) and (*f*) Ti-1473.

of 1023 K to 1573 K (750 °C to 1300 °C) and for a time period in the range of 30 to 120 minutes could remove hydrogen completely, making the hydrogen content in the final product decrease to tens of ppm. The weaker dehydrogenation effect of the present process might be associated with the use of argon atmosphere which is less effective than vacuum for removing the hydrogen from titanium when the hydrogen content is at a ppm level.

B. *Effect of Holding and Extrusion Temperature on Consolidation Level*

There has been some reported research work showing that a higher sintered density of titanium products could be obtained using TiH_2 powder as the starting material instead of pure Ti powder under the same sintering condition,[15,18] suggesting that it is possible to get the Ti or Ti alloys with a good consolidation level at a lower temperature using TiH_2 powder. The present work shows that the relative densities of the three extruded Ti rods are all close to 100 pct, being 99.6, 99.8, and 99.7 pct for the Ti-1273, Ti-1373, and Ti-1473 rods, respectively, suggesting that the presintering during induction heating, holding, and extrusion process is very effective in densifying the Ti powder compacts. There was no cavity formed in the longitudinal sections of the tested and fractured tensile test specimens cut from all the three extruded rods, as shown in Figure 11. This illustrates that the atomic bonding between the powder particles established during presintering by induction heating and holding and plastic deformation during

extrusion is at very high level, even though the holding and extrusion temperature is as low as 1273 K (1000 °C). It should be pointed out that there is still a little amount of hydrogen left in the extruded rods and the good consolidation level at low temperature could be partially attributed to the existence of hydrogen as explained by the decohesion theory introduced by Troiano.[19] The electrons from the hydrogen atoms enter the 3d shells of titanium atoms which are not fully filled with electrons, and this causes the electron concentration of the 3d shells of the titanium atoms to increase. This effect causes the repulsive force among the titanium atoms to increase and reduce the bind force/energy between titanium atoms. The decohesion effect weakened the energy barrier of titanium atom diffusion and increases the diffusivity of titanium atoms, and this in turn can cause a higher sintering rate of Ti powder compact. On the other hand, the surface titanium oxide films are partially reduced through the reduction reaction in the dehydrogenation process as mentioned above and the residual oxide films are rapidly dissolved during heating to 1273 K (1000 °C) or a higher temperature; the reduction of oxide films accelerated the atomic diffusion further. In addition, the volume of powder compacts shrink by over 20 pct due to the lattice contraction when TiH_2 transforms into titanium,[15] which is also beneficial for the densification of the powder compacts.

C. *Effect of Holding and Extrusion Temperature on Microstructure and Mechanical Properties*

The Ti-1273 rod has the highest YS and UTS but the lowest elongation to fracture among the three extruded samples according to the tensile engineering stress–strain curves as shown in Figure 9. Then the YS and UTS decreased when the holding and extrusion temperature increases to 1373 K or 1473 K (1100 °C or 1200 °C). The change of the strength could be explained by the microstructures and H and O contents. In the present study, the holding and extrusion temperature of all the three extruded rods exceeds the α/β phase transition temperature [1155 K (882 °C) for pure titanium], so the release of hydrogen from TiH_2 and the formation of β titanium phase occur at the same time. Since the extrusion cylinder and die are only heated to 773 K (500 °C) and the extruded rods are cooled by the argon atmosphere, the cooling rate of the rods is very fast after extrusion. For Ti-1273 rod, almost all the TiH_2 transforms to titanium after holding and extrusion at 1273 K (1000 °C) as discussed above. The nucleation and growth of α titanium phase maintain a crystallographic orientation relationship with the parent β titanium during cooling to temperatures below the α/β phase transition temperature, and this results in the formation of α lamellae. Because the Ti-1273 rod has the smallest lamellar colonies and thinnest α lamellae, the colony boundary and lamellar boundary strengthening is highest among all the three extruded rods, and this explains why the Ti-1273 rod has the highest YS and UTS among all the three as-extruded rods. When the holding and extrusion temperature increases to 1373 K or 1473 K (1100 °C or 1200 °C), the prior β Ti grains grow up and the cooling time is prolonged compared with that of Ti-1273 rod due to the thermal effect, so the lamellar colonies and α lamellae in the Ti-1373 and Ti-1473 rods grow larger, and the strengthening effect of colony boundaries and interlamellar boundaries weakens, leading to a decrease of YS and UTS. On the other hand, the dehydrogenation process is incomplete with the holding and extrusion temperature of 1273 K (1000 °C), and there is still 0.28 wt pct hydrogen left in Ti-1273 rod according to the chemical analysis shown in Table I and the fact that TiH_2 is detected by the XRD analysis and TEM examination. The measured microhardness of TiH_2 powder particles used in this work is 284 HV, which is significantly higher than that of titanium (219 HV for HDH Ti). This shows that the TiH_2 plates in the microstructure of the Ti-1273 rod can enhance its strength by dispersion strengthening.

Figure 9 shows that the elongation to fracture of the extruded rods changed significantly from 5.4 to 21.0 pct with increasing the holding and extrusion temperature from 1273 K to 1373 K (1000 °C to 1100 °C). From the above discussion on the consolidation level, we have shown that the consolidation levels of all the three extruded rods are quite good, even for the consolidation temperature as low as 1273 K (1000 °C). This suggests

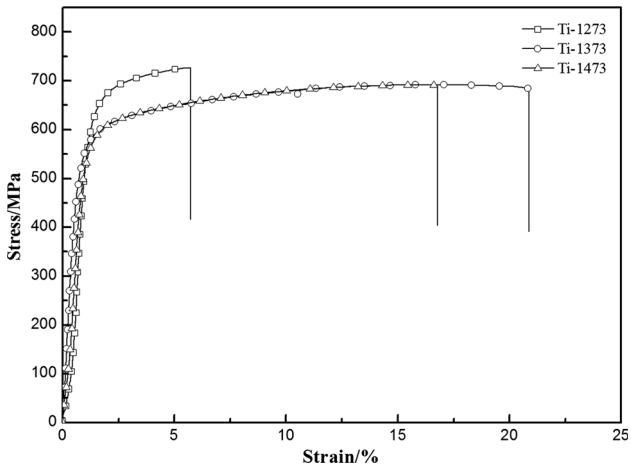

Fig. 9—Tensile engineering stress–strain curves of the specimens cut from the extruded rods.

Table II. Tensile Mechanical Properties of the As-Extruded Rods

Sample	YS (MPa)	UTS (MPa)	Elongation (Percent)
Ti-1273	595.3 ± 11.3	726.6 ± 15.2	5.4 ± 0.7
Ti-1373	536.8 ± 9.5	691.8 ± 11.3	21.0 ± 1.6
Ti-1473	529.3 ± 8.9	673.8 ± 13.7	16.7 ± 1.3

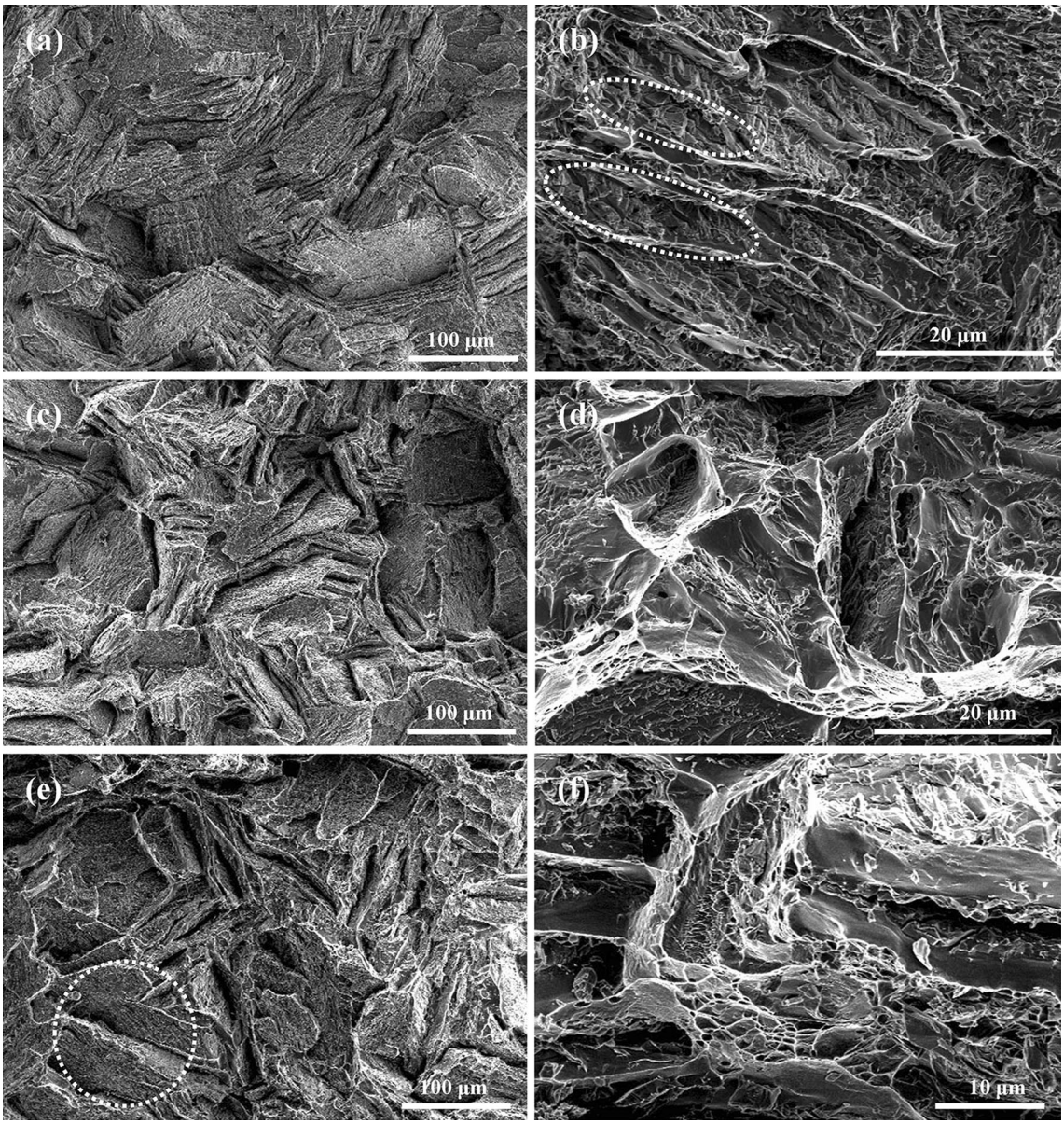

Fig. 10—SEM secondary electron images of the fracture surfaces of the tensile test specimens cut from the as-extruded rods: (*a*) and (*b*) Ti-1273, (*c*) and (*d*) Ti-1373, and (*e*) and (*f*) Ti-1473.

that the significant change of the tensile ductility of the extruded rods is not due to the difference in consolidation level of the samples. The colony size and lamellar thickness can affect the ductility of the samples, and the small colonies and thin α lamellae in the microstructure of the Ti-1273 rod may prevent the extensive movement of dislocations before they are piled up at the colony and lamella boundaries and cause strain concentration and nucleation of cracks, resulting in a low ductility. Based on this consideration, the significant improvement of the tensile ductility of the as-extruded rod with increasing the holding and extrusion temperature from 1273 K to 1373 K (1000 °C to 1100 °C) can be partly attributed to the coarsening of the colonies and α lamellae with increasing the holding and extrusion temperature. On the other hand, there have been some literature reports which show that the TiH_2 phase is intrinsically brittle at temperature lower than 423 K (150 °C),[18,20] so the lower ductility of Ti-1273 rod can also be partly attributed to the existence of TiH_2 plates in the microstructure. The fracture surfaces of the tensile test specimens cut from the Ti-1273 rod are flat and there are micro-cracks existing in some lamellae, as indicated by the circles in Figure 10(b), and these brittle plates are most likely to be TiH_2 plates. Since the dehydrogenation level is improved significantly when the extrusion temperature increases to 1373 K (1100 °C) and there is no TiH_2 phase being detected by the XRD analysis and TEM examination, the improvement of tensile elongation of the Ti-1373 rod could be attributed to the good ductility of titanium without the negative effect of brittle TiH_2 plates. As shown in Figure 10(d), the fracture

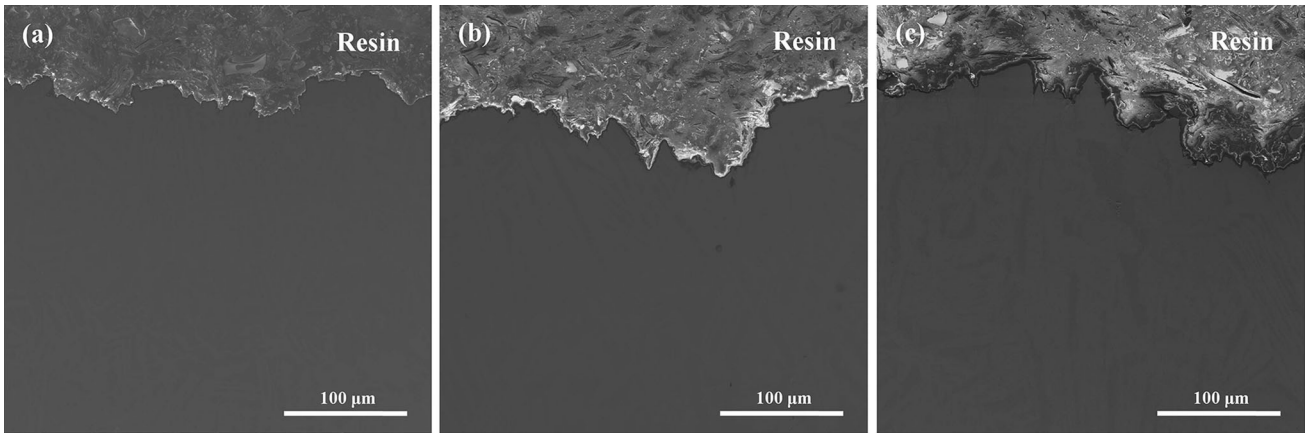

Fig. 11—Longitudinal cross sections below the fracture surfaces of the tensile test specimens cut from the as-extruded rods: (*a*) Ti-1273, (*b*) Ti-1373, and (*c*) Ti-1473.

surfaces of the tensile test specimens cut from the Ti-1373 rod exhibit typical characteristics of ductile fracture such as large dimples, and separation of many lamellae which may be the main reason for failure. For the Ti-1473 rod, the hydrogen content maintains the same level (0.09 wt pct) as that of Ti-1373 rod, so the slight decline of the tensile ductility and the flat regions of the fracture surfaces could be mainly attributed to the increased oxygen content.

V. CONCLUSIONS

Nearly fully dense titanium rods have been fabricated by induction heating, holding, and hot extrusion of TiH_2 powder compacts at temperatures in the range of 1273 K to 1473 K (1000 °C to 1200 °C), with the whole process taking less than 15 min in total.

Almost all the hydrogen in the TiH_2 can be removed after holding and extrusion at 1273 K (1000 °C), the hydrogen content does not decrease further and maintains at 0.09 wt pct when the holding and extrusion temperature increases to 1373 K (1100 °C). The oxygen contents of the extruded rods are all lower than that of the TiH_2 powder used.

All the extruded rods have a lamellar structure consisting of fine α lamellae with random orientations in different lamellar colonies. The thickness of the α lamellae increases from 0.2-1 to 5-8 μm, and the sizes of the lamellar colonies increase from 50-60 to 120-150 μm with the holding and extrusion temperature rising from 1273 K to 1473 K (1000 °C to 1200 °C).

The titanium rod made using the holding and extrusion temperature of 1373 K (1100 °C) has the best tensile ductility (elongation to fracture: 21.0 pct), and its average yield strength and ultimate tensile strength are 536.8 and 691.8 MPa, respectively. The existence of TiH_2 plates and very fine α lamellae in the microstructure of the titanium rod made using the holding and extrusion temperature of 1273 K (1000 °C) could be the reason for its higher strength but much lower tensile ductility.

ACKNOWLEDGMENTS

Funding from the National Natural Science Foundation of China (Project Number: 51271115) and the Ministry of Science and Technology through a 973 project on the scientific basis of fabrication of advanced metal matrix composites (No. 2012CB619600) is gratefully acknowledged.

REFERENCES

1. R.R. Boyer: *Mater. Sci. Eng. A*, 1996, vol. 213, pp. 103–14.
2. R.H. Hu and J.K. Lim: *Mater. Des.*, 2010, vol. 31, pp. 2670–75.
3. V.M. Anokhin, O.M. Ivasishin, and A.N. Petrunko: *Mater. Sci. Eng. A*, 1998, vol. 243, pp. 269–72.
4. O.M. Ivasishin, V.M. Anokhin, and D.G. Savvakin: *Key Eng. Mater.*, 2000, vol. 188, pp. 55–62.
5. I.M. Robertson and G.B. Schaffer: *Powder Metall.*, 2010, vol. 53, pp. 12–19.
6. Z. Yong, M.S. Zheng, H. Hashimoto, and C. Lin: *J. Alloys Compd.*, 2009, vol. 468, pp. 217–21.
7. N. Peillon, J.B. Fruhauf, S. Gourdet, J. Feraille, S. Saunier, and C. Desrayaud: *J. Alloys Compd.*, 2015, vol. 619, pp. 157–64.
8. Y.H. Li, R.B. Chen, G.X. Qi, Z.T. Wang, and Z.Y. Deng: *J. Alloys Compd.*, 2009, vol. 485, pp. 215–18.
9. B. Bertheville, M. Neudenberger, and J.E. Bidaux: *Mater. Sci. Eng. A*, 2004, vol. 384, pp. 143–50.
10. J.L. Bobet, C. Even, and J.M. Quenisset: *J. Alloys Compd.*, 2003, vol. 348, pp. 247–51.
11. C.I. Pascu, O. Gingu, P. Rotaru, I. Vida-Simiti, A. Harabor, and N. Lupu: *J. Therm. Anal. Calorim.*, 2013, vol. 113, pp. 849–57.
12. N.R. Kim, I.Y. Ko, S.W. Cho, W. Kim, and I.J. Shon: *Res. Chem. Intermed.*, 2011, vol. 37, pp. 11–17.
13. S.D. Luo, Y.F. Yang, G.B. Schaffer, and M. Qian: *Scripta Mater.*, 2013, vol. 69, pp. 69–72.
14. G. Chen, P. Cao, and N. Edmonds: *Mater. Sci. Eng. A*, 2013, vol. 582, pp. 117–25.
15. O.M. Ivasishin and D.G. Savvakin: *Key Eng. Mater.*, 2010, vol. 436, pp. 113–21.
16. V. Bhosle, E.G. Baruraj, M. Miranova, and K. Salama: *Metall. Mater. Trans. A*, 2003, vol. 34, pp. 2793–99.
17. Y.F. Yang and D.K. Mu: *Powder Technol.*, 2013, vol. 249, pp. 208–11.
18. F. Prat, M. Grange, J. Besson, and E. Andrieu: *Metall. Mater. Trans. A*, 1998, vol. 29, pp. 1643–51.
19. A.R. Traiano: *Trans. ASM*, 1960, vol. 52, pp. 54–80.
20. K.S. Chan and Y.W. Kim: *Acta Metall. Mater.*, 1995, vol. 43, pp. 439–51.